INSTITUTE OF PHYSICS PUBLISHING JOURNAL OF PHYSICS B: ATOMIC, MOLECULAR AND OPTICAL PHYSICS

J. Phys. B: At. Mol. Opt. Phys. **38** (2005) 3477–3487 doi:10.1088/0953-4075/38/19/002

Experimental study on electron–hexafluoroethane (C_2F_6) collisions in the low- and intermediate-energy ranges

I Iga[1], I P Sanches[1], P Rawat[1], M G P Homem[2,3] and M-T Lee[1]

[1] Departamento de Química, UFSCar, 13565-905 São Carlos, SP, Brazil
[2] Laboratório Nacional de Luz Síncrotron (LNLS), 13083-970 Campinas, SP, Brazil
[3] Departamento de Física, UFSCar, 13565-905 São Carlos, SP, Brazil

Received 10 June 2005, in final form 12 August 2005
Published 12 September 2005
Online at stacks.iop.org/JPhysB/38/3477

Abstract

In this work, we report an experimental study on electron–hexafluoroethane (C_2F_6) collisions in the low- and intermediate-energy ranges. More specifically, absolute differential, integral and momentum-transfer cross sections for elastic e^-–C_2F_6 are measured and reported in the 30–500 eV range. Also, electron-impact partial and total ionization cross sections for this target are reported at incident energies from threshold to 1000 eV. Both measurements were performed using a crossed electron beam–molecular beam geometry. The intensities of the scattered electrons and the signals of ionic fragments are converted to absolute cross sections using the relative flow technique. A comparison between our measured data and the theoretical and other experimental results available in the literature is made.

1. Introduction

Recently, electron collisions with perfluoroalkanes (C_nF_{2n+2}) have received considerable attention, both theoretically and experimentally, due to the role played by these compounds in various fields of application. These species are widely used in new plasma processes [1] and other applications [2]. Particularly in the semiconductor industry, they are indispensable in the formation or deposition of semiconductor films [3, 4]. In particular, hexafluoroethane (C_2F_6) can be used as an etchant gas in the manufacture of semiconductors [5, 6]. For this application, discharge decomposition of this molecule gives rise to fluorine and various neutral radicals, which play a fundamental role for etching SiO_2 and for polymer growth on Si. Moreover, C_2F_6 is also frequently used as gaseous dielectric in the electrical industry [7]. Modelling operational conditions for a particular application requires knowledge of the basic interaction processes and access to comprehensive sets of reliable and accurate experimental cross sections. These cross sections are also important to elucidate some mechanisms and/or to control plasma processing in industry [8].

Despite the intense experimental activity on electron–C_2F_6 interaction during the past two decades (see the review articles of Christophorou and Olthoff [9, 10]), there is still a lack of scattering cross sections for many processes. Specifically for elastic electron scattering by hexafluoroethane, the only measurement of differential (DCS), integral (ICS) and momentum-transfer cross sections (MTCS) was reported by Takagi *et al* [11] in a limited (2–100 eV) incident energy range. For electron-impact ionization processes, partial ionization cross sections (PICS) for $C_2F_5^+$, CF_3^+ and CF^+ fragments, as well as total ionization cross sections (TICS) in the 12.8–130 eV range were measured by Poll and Meischner [12] using a quadrupole mass spectrometer. Using a Fourier transform mass spectrometer, Jiao *et al* [13] also measured PICS of the same ionic fragments from threshold up to 70 eV. The only experimental study on partial ionization of this target covering an extensive energy range was carried out by Basner *et al* [14]. In their work, absolute PICS and TICS of C_2F_6, measured using a time-of-flight mass spectrometer (TOFMS), from threshold to 900 eV are reported. Experimental TICS were also reported by Nishimura *et al* [15] from threshold to 3000 eV. Some discrepancies between the measured PICS [12–14] are observed. In general, the PICS of Basner *et al* [14] lie below the measured values of Jiao *et al* [13] in the overlapping energy range.

Also recently, there has been much activity on the experimental determination of grand total cross sections (TCS) for electron scattering by perfluoroalkanes. Particularly for C_2F_6, TCS were measured by Sueoka *et al* [16] in the 0.8–600 eV energy range, by Sanabia *et al* [17] in the 0–20 eV energy range, by Szmytkowski *et al* [18] in the 0.5–250 eV energy range, by Ariyasinghe [19] in the 100–1500 eV energy range, and more recently, by Nishimura *et al* [20] in the 1.5–3000 eV energy range. Also in this case, some inconsistencies are seen among the measured data. For example, the TCS reported by Sueoka *et al* and Sanabia *et al* lie substantially below those measured by Szmytkowski *et al* and Nishimura *et al*, particularly at higher incident energies.

Considering the importance of this molecule in various fields of application, more experimental determination of several cross sections would certainly be interesting, not only to confirm the existing results but also to produce new data, particularly extensive to higher incident energies. Also from the fundamental point of view, more experimental results covering a wide range of incident energies may stimulate interest for theoretical investigations. In this paper, we report an experimental study on elastic electron scattering by C_2F_6 as well as on electron-impact ionization of this molecule. More specifically, absolute DCS, ICS and MTCS in the 30–500 eV range for elastic scattering, as well as PICS and TICS from threshold up to 1000 eV for C_2F_6 are reported. In the present work, the intensities of the scattered electron signals and of the ionic-fragment signals are converted to absolute cross sections by using the relative flow technique (RFT) [21–23]. ICS and MTCS are derived from the DCS measured in the 10–130° angular range and extrapolated to forward and backward directions. In addition, an estimate of TCS is made by adding up the present ICS and TICS. As observed by Joshipura *et al* [24], ionization channel dominates the inelastic processes at high incident energies. The TICS correspond to about 80% of the total inelastic cross section at energies around 100 eV and go to near 100% for energies above 300 eV. Therefore, a comparison of our TCS with the experimental TCS [16, 18–20] may provide an estimate of the importance of other inelastic channels (excitation and dissociation) but ionization. Also, our estimated TCS at high energies may serve as a check of the reliability of the existing experimental TCS.

The organization of this paper is as follows. In section 2, some experimental details are presented. Finally, in section 3, our experimental results are compared with existing theoretical and/or experimental data.

2. Experimental details

2.1. Elastic scattering

Details of our experimental set-up and procedure for elastic DCS determinations have already been presented in our previous works [25, 26]. Briefly, a crossed electron beam–molecular beam geometry is used to measure the relative distribution of the scattered electrons as a function of the scattering angle at a given incident electron energy. The scattered electrons are energy filtered by a retarding-field energy selector with a resolution of about 1.5 eV. With this resolution, it is sufficient to distinguish inelastically scattered electrons resulting from electronic excitation for this molecule; nevertheless, it is unable to separate those from vibrational excitation processes. Therefore, our measured DCS are indeed vibrationally summed. During the measurements, the working pressure in the vacuum chamber is around 5×10^{-7} Torr. The recorded scattering intensities are converted into absolute elastic DCS using the RFT [21–23]. Accordingly, the DCS for a gas under determination (x) can be related with known DCS of a secondary standard (std) as

$$(\mathrm{DCS})_x = (\mathrm{DCS})_{\mathrm{std}} \frac{I_x}{I_{\mathrm{std}}} \frac{n_{\mathrm{std}}}{n_x} \left(\frac{M_{\mathrm{std}}}{M_x} \right)^{\frac{1}{2}}, \tag{1}$$

where I is the scattered electron intensity, n is the flow rate and M is the molecular weight. The above equation is valid if the beam profiles (density distribution) of both gases, x and std, are closely the same. The details of the application of RFT can be found in our recent article [27].

In the present study, Ar is used as the secondary standard. Absolute DCS of Jansen *et al* [28] in the 100–500 eV energy range and those of Panajotović *et al* [29] at 30 and 60 eV are used to normalize our data. Details of the analysis of experimental uncertainties have also been given elsewhere [25]. They are estimated briefly as follows. Uncertainties of random nature such as pressure fluctuations, electron beam current readings, background scattering, etc, are estimated to be less than 2%. These contributions combined with the estimated statistical errors give an overall uncertainty of 4% in the relative DCS for each gas. Also, the experimental uncertainty associated with the normalization procedure is estimated to be 5.7%. These errors combined with the quoted errors [28, 29] in the absolute DCS of the secondary standard provide overall experimental uncertainties of 11% in the 100–500 eV range and 23% elsewhere in our absolute DCS. The absolute DCS were determined in the 10–135° angular range. In order to obtain ICS and MTCS, an extrapolation procedure was adopted to estimate DCS at scattering angles out of that range. The extrapolation was carried out manually. The overall errors on ICS and MTCS are estimated to be 22% in the 100–500 eV range and 30% below 100 eV.

2.2. Ionization

The experimental apparatus and method used for the present investigation on the ionization of C_2F_6 have already been detailed in our previous studies [30] and will only be briefly outlined. As in the elastic-scattering studies, a cross-beam arrangement was used to measure the PICS. The C_2F_6 beam was prepared by flowing the gas through a capillary array. A pulsed electron beam with pulse width of around 100 ns and pulse frequency of 10 kHz is used in our experiment. After the electron–molecule interaction, the resulting ionic fragments are extracted towards the TOFMS [30] that is located perpendicularly to the plane formed by the electron and molecular beams. Since the fragment ions can be created with appreciable kinetic energies [31, 32], it is essential to extract them out of the collision region with a high

Table 1. Experimental DCS, ICS and MTCS (in 10^{-16} cm^2) for elastic e$^-$–C_2F_6 scattering.

	E_0 (eV)			
Angle (°)	30	60	100	150
0	[4.25(1)][a]	[1.96(2)]	[1.62(2)[b]]	[1.53(2)]
8		7.61(1)	5.69(1)	4.83(1)
10		5.55(1)	3.90(1)	3.12(1)
15	1.92(1)	2.26(1)	1.19(1)	6.57(0)
20	1.23(1)	6.50(0)	2.56(0)	3.13(0)
25		2.34(0)	2.44(0)	2.76(0)
30	5.24(0)	2.05(0)	2.12(0)	1.74(0)
35		1.94(0)	1.40(0)	1.01(0)
40	9.90(−1)	1.65(0)	9.40(−1)	6.20(−1)
45		1.19(0)	6.10(−1)	4.80(−1)
50	1.68(0)	9.14(−1)	4.20(−1)	4.60(−1)
60	1.85(0)	5.60(−1)	3.40(−1)	3.00(−1)
70	1.21(0)	3.60(−1)	2.60(−1)	1.50(−1)
80	7.30(−1)	2.20(−1)	1.60(−1)	1.10(−1)
90	6.70(−1)	2.00(−1)	1.30(−1)	1.20(−1)
100	5.20(−1)	2.20(−1)	1.30(−1)	1.20(−1)
110	5.60(−1)	2.60(−1)	1.90(−1)	1.40(−1)
120	7.10(−1)	4.60(−1)	2.70(−1)	1.90(−1)
130	1.38(0)	6.90(−1)	3.70(−1)	2.40(−1)
180	[4.00(0)]	[1.64(0)]	[1.00(0)]	[4.88(−1)]
ICS	2.81(1)	2.49(1)	1.70(1)	1.49(1)
MTCS	1.80(1)	1.01(1)	5.01(0)	3.18(0)

	200	300	400	500
0	[1.85(2)]	[2.06(2)]	[2.04(2)]	[2.03(2)]
8	3.78(1)	2.60(1)	1.91(1)	1.07(1)
10	1.97(1)	8.86(0)	6.26(0)	4.90(0)
15	3.52(0)	3.63(0)	4.63(0)	4.53(0)
17				3.47(0)
20	3.51(0)	2.94(0)	2.80(0)	2.02(0)
22				1.54(0)
25	2.38(0)	1.47(0)	1.33(0)	1.38(0)
27				1.34(0)
30	1.28(0)	8.70(−1)	1.24(0)	1.17(0)
35	7.60(−1)	8.50(−1)	8.80(−1)	5.00(−1)
77				4.20(−1)
40	6.40(−1)	6.60(−1)	4.30(−1)	3.00(−1)
45				2.30(−1)
50	6.10(−1)	2.20(−1)	2.20(−1)	1.90(−1)
55	4.40(−1)	1.70(−1)	1.90(−1)	
60	1.90(−1)	1.50(−1)	1.40(−1)	1.38(−1)
65		1.20(−1)		
70	1.30(−1)	1.00(−1)	1.00(−1)	7.20(−2)
80	1.20(−1)	8.40(−2)	7.30(−2)	6.40(−2)
90	1.10(−1)	7.40(−2)	6.50(−2)	6.00(−2)

extraction field, which is generated by applying appropriate voltages to a pair of wire meshes, symmetrically placed on the sides of the collision region. In order to avoid interference of the applied extraction field on the electron beam, a pulsed extraction method [33] is used in our experiment. Basically, the extraction potential is pulsed in synchronization with the pulsed

Table 1. (Continued.)

	E_0 (eV)			
Angle(°)	200	300	400	500
100	1.20(−1)	7.00(−2)	5.60(−2)	3.50(−2)
110	1.20(−1)	7.00(−2)	4.90(−2)	3.50(−2)
120	1.30(−1)	7.20(−2)	5.00(−2)	3.30(−2)
130	1.60(−1)	8.00(−2)	4.90(−2)	3.00(−2)
180	[3.04(−1)]	[9.50(−2)]	[4.20(−2)]	[3.20(−2)]
ICS	1.31(1)	1.00(1)	8.71(0)	6.30(0)
MTCS	2.46(0)	1.36(0)	9.49(−1)	8.23(−1)

[a] [x] means extrapolated values.
[b] 1.62(2) means 1.62×10^2.

electron beam. During the passage of a pulse of electrons through the collision region, the voltage on the pair of grids is kept at 0 V. However, 100 ns after the electron pulse leaves the collision region (trapped by a Faraday cup), a voltage of about 200 V is applied to the grids (+200 V on the repeller side and −200 V on the side facing TOFMS) by a fast pulse generator. This extraction ensures a complete collection of ions with energies up to 20 eV [34]. After being analysed by the TOFMS, the ionic fragments are detected by a charged particle detector 'channeltron'. Because, in general, the transmission efficiency of mass spectrometers depends on mass-to-charge ratios, we calibrated our mass spectrometer system (including ion source, TOF tube and the charged particle detector) by utilizing various rare gases and other gases for which the ionization cross sections are accurately known. It was found that the transmission efficiency of ions in our system was practically independent of their mass-to-charge ratios. In addition, the intensities of each fragment ion seen in the TOF spectrum were independently recorded in the multichannel scaler (MCS), as a function of the electron beam energy, from threshold of ionization to 1000 eV. Lately, these intensities are converted to PICS by using the RFT. The experimental PICS of Straub *et al* [35] for Ar^+ at an impact energy of 500 eV was used as the secondary standard.

The estimate of experimental uncertainties contributing to various steps of the measurements is described as follows. The uncertainties in the relative cross sections of each fragment ion were calculated from the standard deviation of five independent measurements of ionization efficiency curves. The resulting uncertainties are 5% for the $C_2F_5^+$ and CF_3^+, 8% for the CF_2^+ and CF^+, and 15% for the C^+ and F^+ fragments, respectively. Errors of the flow rate measurements are estimated to be less than 2%, whereas an uncertainty of the cross sections of the reference gas of 3.5% is also considered. The resulting relative errors in the absolute partial ionization cross sections are, therefore, 7% for the $C_2F_5^+$ and CF_3^+, 9% for the CF_2^+ and CF^+, and 16% for the C^+ and F^+ fragments, respectively. The TICS are obtained by summing up the individual PICS.

3. Results and discussion

3.1. Elastic scattering

The present experimental data of DCS, ICS and MTCS, obtained in the 30–500 eV energy range, are presented in table 1. Some representative results of DCS at selected incident energies are also plotted in figure 1, along with the existing experimental data [11] and with the present calculated DCS using the independent-atom model (IAM). In these calculations,

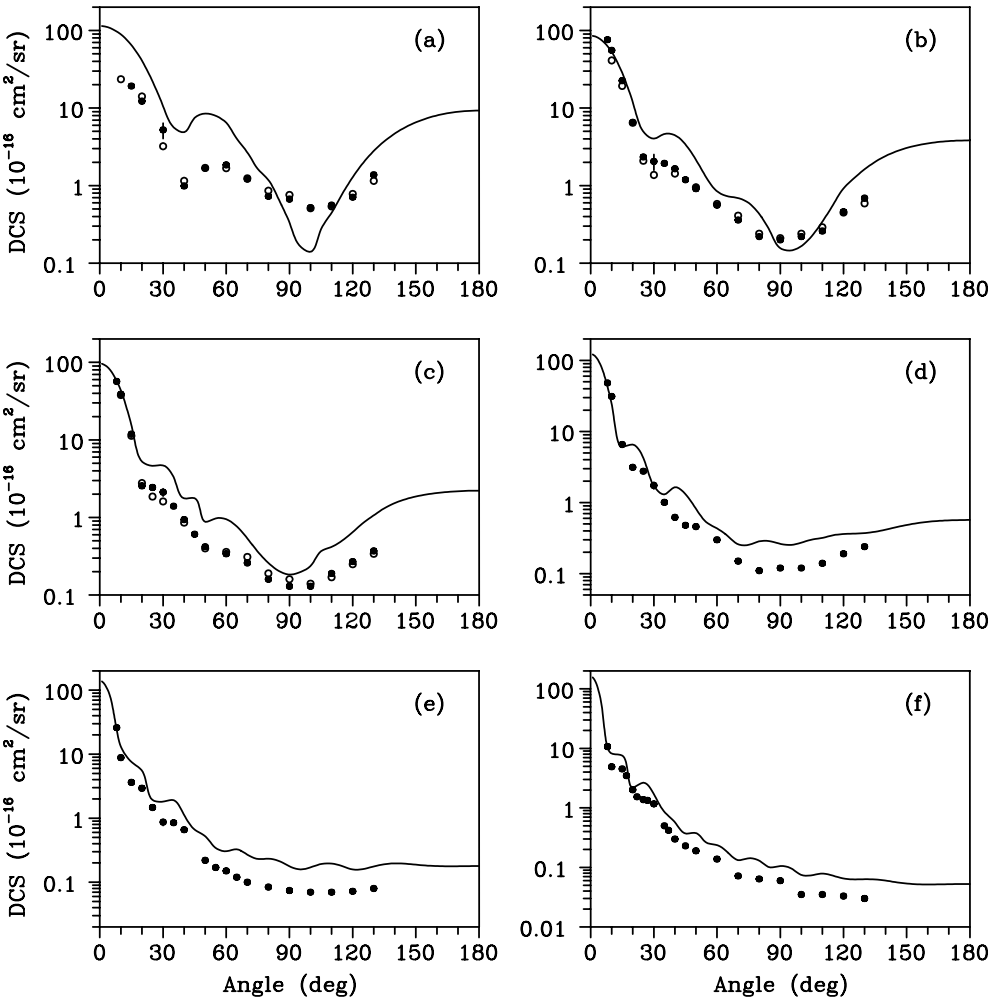

Figure 1. DCS for elastic e^-–C_2F_6 scattering at incident energies of (a) 30 eV, (b) 60 eV, (c) 100 eV, (d) 200 eV, (e) 300 eV and (f) 500 eV. Full circles present experimental results, open circles present experimental results of Takagi *et al* [11] and solid line presents calculated results using the IAM.

the electron-scattering amplitudes for individual carbon and fluorine atoms are obtained within the partial-wave framework [36] using a Yukawa type of potential [37]. The amplitudes for electron–C_2F_6 scattering are then obtained via

$$f_{\mathrm{mol}} = \sum_{i=1}^{N} f_i \, \mathrm{e}^{\mathrm{i}\vec{q}\vec{R}_i}, \tag{2}$$

where f_i are the atomic scattering amplitudes, N is the number of atoms, $\vec{R}_i$ is the position vector of atom i and $\vec{q}$ is the momentum transfer of the scattering electron during the collision.

Our experimental DCS at 30, 60 and 100 eV are in good agreement, both qualitatively and quantitatively, with the measured data of Takagi *et al* [11]. This fact itself is very interesting since the measurements were performed independently by our group and Takagi *et al* with different energy analysers and secondary standards. Therefore, this good agreement may

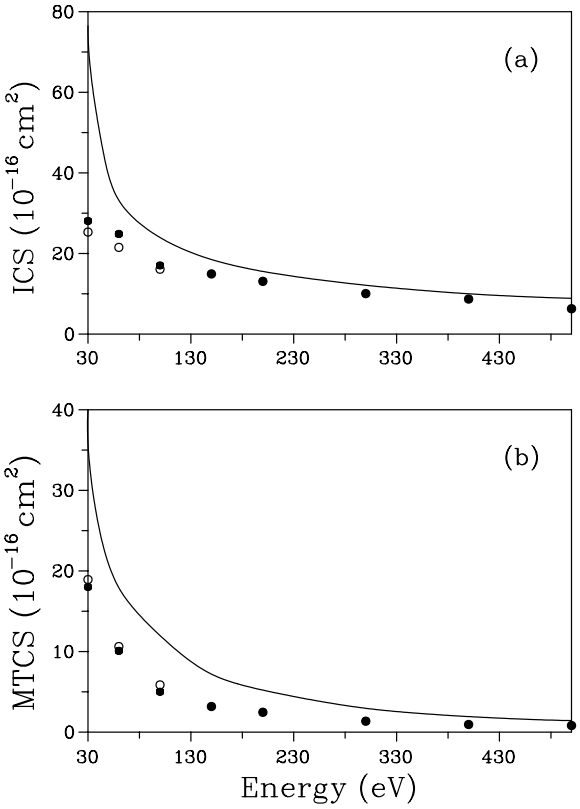

Figure 2. ICS (a) and MTCS (b) for elastic e^-–C_2F_6 scattering. Full circles present experimental results, open circles present experimental results of Takagi *et al* [11] and solid line presents calculated results using the IAM.

reflect the reliability of the DCS of both groups. The calculated values using the IAM agree qualitatively with our measured data in the entire energy range covered herein. Quantitatively, best agreement between the present experimental and IAM DCS is seen at around 60 eV. At higher energies, the IAM calculations overestimate the DCS at intermediate and large scattering angles, probably due to the neglect of the absorption effects.

In figure 2, we present our experimental ICS and MTCS, obtained via numerical integration of our DCS that were extrapolated manually towards both the forward and backward directions. The experimental data of Takagi *et al* [11] at 30, 60 and 100 eV and the theoretical IAM data are also shown for comparison. Again, there is a good agreement between the two sets of experimental results in the overlapping energy range. The small discrepancy in ICS is probably due to the different extrapolated DCS towards the forward direction. The calculated ICS and MTCS agree qualitatively with the experimental data. Fairly good quantitative agreement is also seen for ICS at energies above 150 eV and for MTCS at 200 eV and above.

3.2. Ionization

In figures 3(a) and (b), we present our experimental PICS for the $C_2F_5^+$ and CF_3^+ ionic fragments, respectively, produced from electron impact on C_2F_6 in the energy range from threshold to 1000 eV. The corresponding experimental data of Poll and Meischner [12], Jiao *et al* [13] and

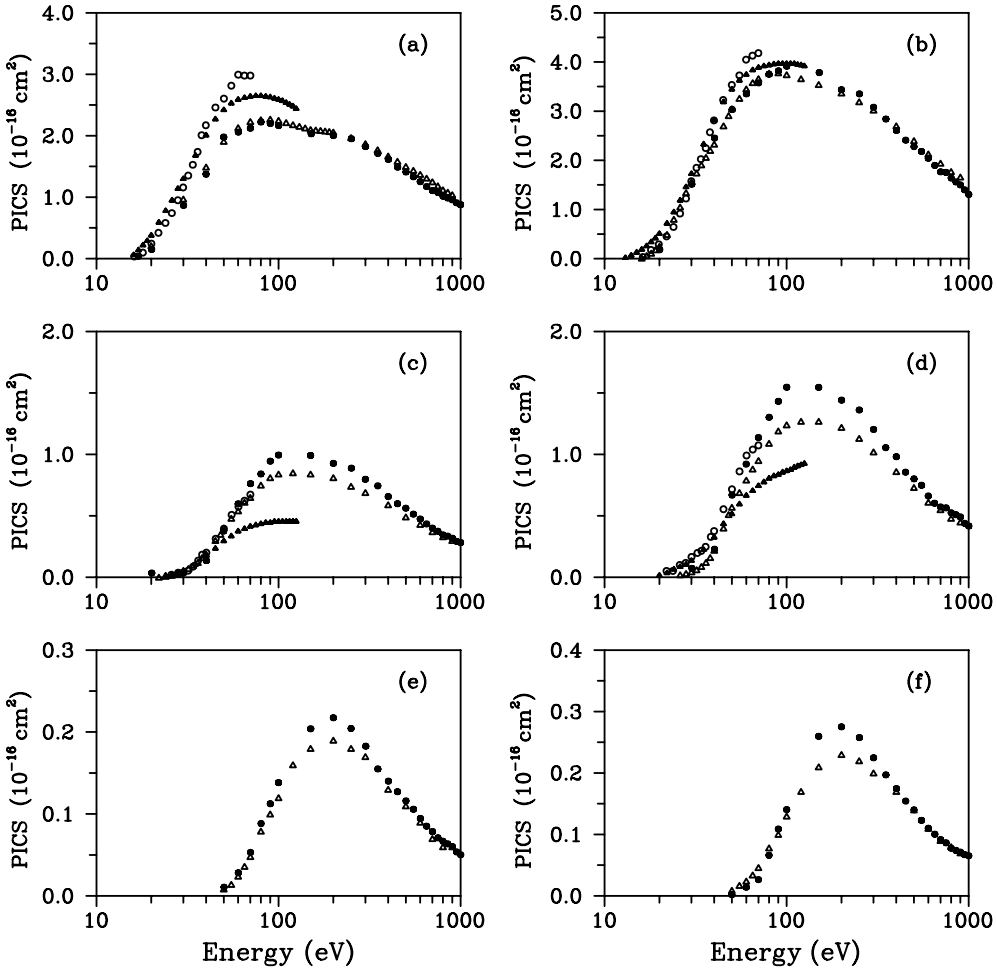

Figure 3. PICS for (a) $C_2F_5^+$, (b) CF_3^+, (c) CF_2^+, (d) CF^+, (e) C^+ and (f) F^+ fragments, produced from electron impact on C_2F_6. Full circles present experimental results, open circles present experimental results of Jiao *et al* [13], full triangles present measured data of Poll and Meischner [12] and open triangles present measured data of Basner *et al* [14].

Basner *et al* [14] are also shown for comparison. For the $C_2F_5^+$ fragment, our measured PICS agree very well with those of Basner *et al* [14] in the entire energy range. On the other hand, the experimental results of Poll and Meischner and Jiao *et al* overestimate the PICS near the maximum. For the CF_3^+ fragment, our experimental PICS are again in very good agreement with those of Basner *et al* in the energy range where the comparison is made. A generally good agreement is also seen between our PICS and those of Poll and Meischner and Jiao *et al* for the production of this fragment.

Figures 3(c) and (d) show our experimental PICS for the production of the CF_2^+ and CF^+ ionic fragments, respectively, from electron–C_2F_6 collisions. Again, comparison is made with the experimental data of Poll and Meischner [12], Jiao *et al* [13] and Basner *et al* [14]. For the CF_2^+ fragment, our experimental PICS are in good agreement with those of Jiao *et al* and with the measured data of Basner *et al* except at the region of the maximum, where our PICS are about 10% larger. Nevertheless, this discrepancy lie within the estimated experimental

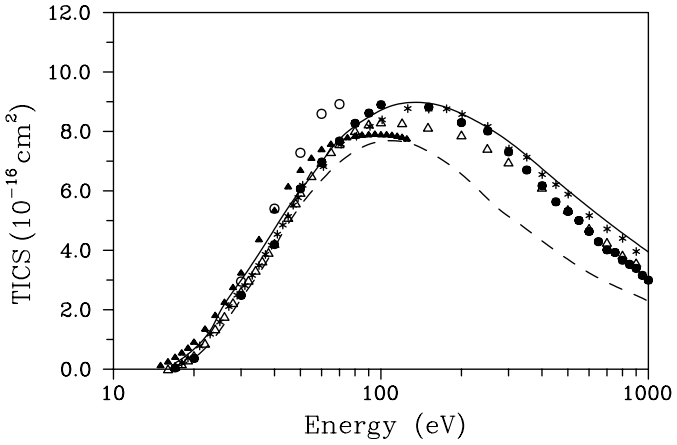

Figure 4. TICS for electron impact on C_2F_6. Full circles present experimental results, open circles present experimental results of Jiao *et al* [13], full triangles present measured data of Poll and Meischner [12], open triangles present measured data of Basner *et al* [14], asterisks present measured data of Nishimura *et al* [15], solid line presents BEB TICS of Nishimura *et al* [15] and dashed line presents DM TICS of Deutsch *et al* [38].

uncertainties. On the other hand, the measured PICS of Poll and Meischner [12] lie well below all other measured data, particularly in the 60–130 eV range. The same behaviour is again observed for the production of the CF^+ fragment, shown in figure 3(d), where the experimental PICS of Poll and Meischner lie again well below other experiments. This fact may indicate that the experimental set-up of these authors has some discrimination in the detection of energetic ions since both CF_2^+ and CF^+ fragments are energetic.

Figures 3(e) and (f) compare the present experimental PICS for the production of the C^+ and F^+ ionic fragments, respectively, with the corresponding data of Basner *et al* [14]. In general, there is a good agreement, both qualitatively and quantitatively, between our data and those of Basner *et al*. The small differences seen near the maxima lie within the estimated experimental uncertainties. It is well known that the measurement of the PICS for production of C^+ and F^+ ions by electron impact on C_2F_6 is difficult because both fragments are energetic. Moreover, their PICS are small. Therefore, this good agreement is encouraging and seems to confirm the reliability of both measurements.

Finally, in figure 4, we present our TICS obtained by adding up the PICS of individual ionic fragments. The small contributions of some fragments such as $C_2F_4^+$, C_2F^+ and C_2^+, accounted for in the paper of Basner *et al* [14], are not included in the present study. For comparison, we also show the experimental TICS for electron-impact ionization of C_2F_6 of Basner *et al* [14], Poll and Meischner [12], Jiao *et al* [13] and Nishimura *et al* [15], as well as the calculated TICS of Nishimura *et al* [15] using the binary-encounter-Bethe (BEB) model and those of Deutsch *et al* [38] using the DM model. In general, all the experimental data agree reasonably well with each other. Particularly, it is interesting to note the good agreement between the TICS of Poll and Meischner [12] and our data, despite the significant discrepancies seen in the comparison of individual PICS. It is probably due to some kind of compensation because of the overestimation of the PICS for production of $C_2F_5^+$ and CF_3^+ fragments and underestimation of CF_2^+ and CF^+ fragments in their work. The calculated TICS of Nishimura *et al* [15] using the BEB model and those calculated by Antony *et al* [39] (not shown) also agree very well with the present data. Nevertheless, the DM calculation underestimates significantly the TICS, particularly at incident energies above 100 eV.

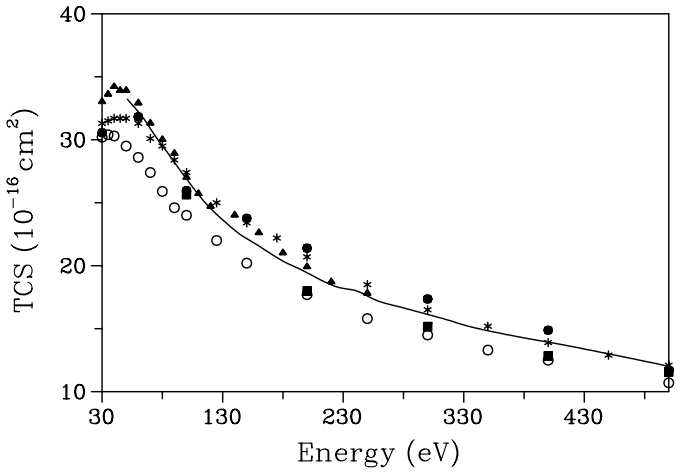

Figure 5. TCS for e^-–C_2F_6 scattering. Full circles present estimated TCS, asterisks present measured data of Nishimura *et al* [20], open circles present experimental TCS of Sueoka *et al* [16], full triangles present experimental TCS of Szmytkowski *et al* [18], full squares present experimental TCS of Ariyasinghe [19] and solid line presents calculated data of Antony *et al* [39].

3.3. Total cross section

In this section, we present our results of TCS, estimated by adding up the present experimental TICS to our elastic ICS. These estimated TCS are shown in figure 5, along with some experimental TCS available in the literature [16, 18–20]. The calculated TCS of Antony *et al* [39], using a spherical complex potential formalism, are also shown for comparison. A general good agreement between our estimated TCS and the experimental results of Szmytkowski *et al* [18] and Nishimura *et al* [20] is seen at incident energies above 100 eV. The calculated values of Antony *et al* [39] also agree very well with our estimated TCS. However, some discrepancies are seen between our TCS and the experimental results of Sueoka *et al* [16] and Ariyasinghe [19]. Particularly, the experimental TCS of Sueoka *et al* [16] lie systematically below all other data. The good agreement between our TCS and the experimental data of Szmytkowski *et al* [18] and Nishimura *et al* [20] seems to reinforce that the ionization channel is dominant among all inelastic processes at high incident energies. On the other hand, at energies below 100 eV, our estimated TCS are slightly lower than the experimental values of Szmytkowski *et al* [18], this difference may be attributed to the electronic excitation processes.

Acknowledgments

The authors would like to thank Dr S K Srivastava and Professor G C King (The University of Manchester) for the useful discussion for the development of our experimental set-up during their visits to São Carlos supported by the International Cooperation Programmes: CNPq–NSF and CNPq–The British Council. This research was partially supported by the Brazilian agencies CNPq and FAPESP.

References

[1] Haond M 1992 *European Patent Application* EP487380
[2] Iriyama Y and Yasuda H 1992 *J. Polym. Sci.* A **30** 1731

[3] Reinhardt K 1992 *Proc. Electrochem. Soc.* **92** 133
[4] Op de Beeck M, Goethais M and Van den Hove L 1992 *J. Electrochem. Soc.* **139** 2644
[5] Urashima K, Kostov K G, Chang J S, Okayasu Y, Iwaizumi T, Yoshimura K and Kato T 2001 *IEEE Trans. Industry Appl.* **37** 1456
[6] Miller P A and Greenberg K E 1992 *Appl. Phys. Lett.* **60** 2859
[7] Božin S E and Goodyear C C 1968 *J. Appl. Phys.* D **1** 327
[8] Morgan W L 2000 *Adv. At. Mol. Opt. Phys.* **43** 79
[9] Christophorou L G and Olthoff J K 1998 *J. Phys. Chem. Ref. Data* **27** 1
[10] Christophorou L G and Olthoff J K 1999 *J. Phys. Chem. Ref. Data* **28** 967
[11] Takagi T, Boesten L, Tanaka H and Dillon M A 1994 *J. Phys. B: At. Mol. Opt. Phys.* **27** 5389
[12] Poll H U and Meischner J 1987 *Contrib. Plasma Phys.* **27** 359
[13] Jiao C Q, Garscadden A and Haaland P D 1999 *Chem. Phys. Lett.* **310** 52
[14] Basner R, Schmidt M, Denisov D, Lopata P, Becker K and Deutsch H 2002 *Int. J. Mass Spectrom.* **214** 365
[15] Nishimura H, Huo W M, Ali M A and Kim Y-K 1999 *J. Chem. Phys.* **110** 3811
[16] Sueoka O, Makochekanwa C and Kawate H 2002 *Nucl. Instrum. Methods* B **192** 206
[17] Sanabia J E, Cooper G D, Tossel J A and Moore J H 1998 *J. Chem. Phys.* **108** 389
[18] Szmytkowski Cz, Mozejko P, Kasperski G and Ptasińska-Denga E 2000 *J. Phys. B: At. Mol. Opt. Phys.* **33** 15
[19] Ariyasinghe W M 2003 *Radiat. Phys. Chem.* **68** 79
[20] Nishimura H, Nishimura F, Nakamura Y and Okuda K 2003 *J. Phys. Soc. Japan* **72** 1080
[21] Srivastava S K, Chutjian A and Trajmar S 1975 *J. Chem. Phys.* **63** 2659
[22] Khakoo M A and Trajmar S 1986 *Phys. Rev.* A **34** 138
[23] Tanaka H, Ishikawa T, Masai T, Sagara T, Boesten L, Takekawa M, Itikawa Y and Kimura M 1998 *Phys. Rev.* A **57** 1798
[24] Joshipura K N, Vinodkumar M and Patel P M 2000 *J. Phys. B: At. Mol. Opt. Phys.* **34** 509
[25] Iga I, Lee M T, Homem M G P, Machado L E and Brescansin L M 2000 *Phys. Rev.* A **61** 227081
[26] Rawat P, Iga I, Lee M T, Brescansin L M, Machado L E and Homem M G P 2003 *Phys. Rev.* A **68** 052711
[27] Iga I, Rawat P, Sanches I P, Lee M T and Homem M G P 2005 *J. Phys. B: At. Mol. Opt. Phys.* **38** 2319
[28] Jansen R H J, de Heer F J, Luyken H J, van Wingerden B and Laauw H J B 1976 *J. Phys. B: At. Mol. Phys.* **9** 185
[29] Panajotović R, Filipović D, Marinković B, Pejčev V, Kurepa M and Vušković L 1997 *J. Phys. B: At. Mol. Opt. Phys.* **30** 5877
[30] Iga I, Sanches I P, Srivastava S K and Mangan M 2001 *Int. J. Mass Spectrom.* **208** 159
[31] Bruce M R and Bonham R A 1993 *Int. J. Mass Spectrom.* **123** 97
[32] Poll H U, Winkler K, Margreiter D, Gill V and Märk T 1992 *Int. J. Mass Spectrom.* **112** 1
[33] Krishnakumar E and Srivastava S K 1988 *J. Phys. B: At. Mol. Opt. Phys.* **21** 1055
[34] Sanches I P 1999 *Master's Dissertation* Universidade Federal de São Carlos
[35] Straub H C, Renault P, Lindsay B G, Smith K A and Stebbings R F 1995 *Phys. Rev.* A **52** 1115
[36] Bransden B H 1983 *Atomic Collision Theory* (New York: Benjamin-Cummings)
[37] Cox H L Jr and Bonham R A 1967 *J. Chem. Phys.* **47** 2599
[38] Deutsch H, Becker K, Matt S and Märk T D 2000 *Int. J. Mass Spectrom.* **197** 37
[39] Antony B K, Joshipura K N and Mason N J 2005 *J. Phys. B: At. Mol. Opt. Phys.* **38** 189